



Research article

Lateral crashworthiness response of bombyx mori fibre/glass–fibre/epoxy hybrid composite cylindrical tubes-experimental

Albert Uchenna Ude^{1,*} and Che Husna Azhari²

¹ Department of Mechanical, Energy and Industrial Engineering, Faculty of Engineering, Botswana International University of Science and Technology, Private Bag 16 Palapye, Botswana

² Department of Mechanical and Materials Engineering, Faculty of Engineering and Built Environment, The National University of Malaysia, UKM, 43600 Bangi, Selangor-Malaysia

* **Correspondence:** Email: udea@biust.ac.bw; Tel: +26775957014; Fax: +2674900102.

Abstract: Experimental studies were undertaken to investigate the effect of reinforced fibre hybridization on the crushing characteristics of quasi-static laterally compressed cylindrical composite tubes. Woven glass fibre (GF) and woven bombyx mori fibre (B.mori) were used as reinforcements and industrial epoxy was used as the matrix material to fabricate the reinforced hybrid composite specimen. Three sets of specimen were fabricated, (1) glass fibre/epoxy (2) B.mori fibre/epoxy and (3) GF/B.mori/epoxy hybrid composite, to clearly ascertain the effect of reinforced fibre hybridization. Load-displacement curves and specimen's deformation histories were used to analyze energy absorption and load carriability. The length of each specimen was 80 mm, three specimens were tested from each set and an average value recorded. Generally, the results showed that the hybrid composite tube specimen performed better when compared with the other tubes.

Keywords: hybrid; textile; reinforced fibres; composite; energy absorption

1. Introduction

Owing to properties such as strength-to-weight-ratio, corrosion inactiveness, stiffness, easy formability and other, composite structures has find its way into many manufacturing industries including but not limited to automobiles, aerospace, marine, sports and construction. Presently, their degree of acceptance and percentage of usage in fabrication of aerospace component parts has increased rapidly in the last decade; many automobile manufacturers have also increased their usage

of composite component parts in their automobiles, citing government legislations, environment friendly materials, light weight, as well as aesthetics, to mention but a few. During the in-service time, unfortunately these component parts are prone to different kind of stresses and loadings. Failures due to induced stresses via tensile and compression loading on the composite structures has caused devastating damages in the past and has remained a hot research focus for some decades now. Researchers all around the globe are constantly in search of new materials with superior material characteristics or new approach that can answer to some drawbacks encountered during applications. One such drawback in the application of composites is the unpredictable failure characteristics of composites structures during external impact. Impact on a composite structure may be classified in the range of its velocity as, low, medium or high velocity; and in-terms of surface as axial, or transverse impact.

Literature review reveals that many research works have been carried out to investigate axial crushing behaviors of varied composite tubes of varied geometries [1–10], fewer investigations have been carried out on the lateral crashworthiness performance of composite structures [11–14] and no report was recorded on the lateral crashworthiness performance of bombyx mori silk fibre or bombyx mori silk fibre/glass–fibre/epoxy hybrid composite cylindrical tubes, the reason for which this investigation was carried out. Sebaey and Mahdi [15] reported that if an external object strikes a composite structure perpendicular to its surface, it can damage both its static and fatigue load-bearing capacities. Absobaia et al. [14] reported that segmented cotton fibre/epoxy and carbon fibre/epoxy composite tubes, are effective crushing elements when subjected to laterally deformation loading. They also reported that tissue mat glass fibres composite tubes suffer from low energy absorption. It was also reported by Majid et al. that stiffening the composite cylindrical shells with lozenge grid stiffeners can increase the specific energy absorption almost twice in comparison with the unstiffened composite shell; the grid-stiffened structures compressed between two rigid flat platens also had the highest specific energy absorption when compared with the unstiffened structures compressed by the cylindrical indenter [16]. Other recent investigations on laterally deformed composites includes [17–20]. It is well established that composite structures are very susceptible to external impact loads. Axial deformation of composites structures generates greater resistance to fracture than lateral deformation due to the reinforced laminate arrangements. This investigation was carried out to improved lateral strength deformation in composite materials without compromising their weight. Some of the examples where composite structures are subjected to lateral deformations include oil and water pipe lines; airplane frames structures and recently, some automobile structures. No investigation has been carried out on the response of bombyx mori/epoxy composite cylindrical tubes deformed laterally.

This investigation is then focused on the quasi-static lateral impact response of varied cylindrical composite tubes. Their responses were measured via peak load, energy absorption, crushing efficiency as well as the nature of tube fragmentation. The test results were displayed and analyzed in subsequent sections below.

2. Materials and methods

The materials used in this investigation were glass fibre, woven bombyx mori natural silk fibres, supplied by Loxevi silk; epoxy resin type (DER 331) and hardener type (905-35). The method of fabrication was by mandrel assisted hand lay-up, three categories of specimen were fabricated (1)

glass fibre reinforced epoxy composite cylindrical tubes, (2) bombyx mori reinforced epoxy composite cylindrical tubes, (3) glass fibre/bombyx mori fibre hybrid reinforced epoxy composite cylindrical tubes. The length of each composite tube specimen was 80 mm, with an internal diameter of 65 mm and thickness of 15 mm respectively. The samples of bombyx mori fibre and glass fibre used were shown in Figure 1, while the schematics diagrams of the cylindrical composite specimens, used in the test were shown in Figure 2. All composite samples were manufactured at an ambient temperature.

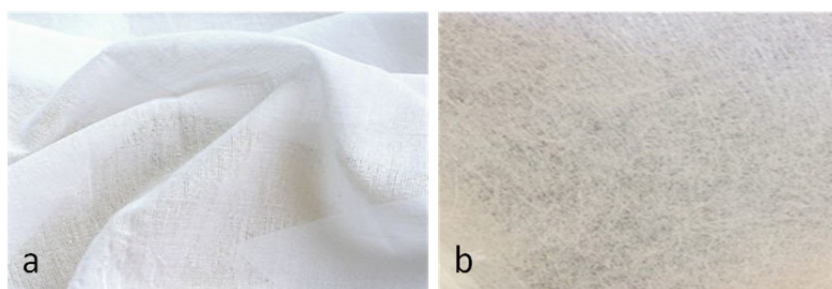


Figure 1. Samples of fibres used (a) natural fibre (B.mori), (b) glass fibre.

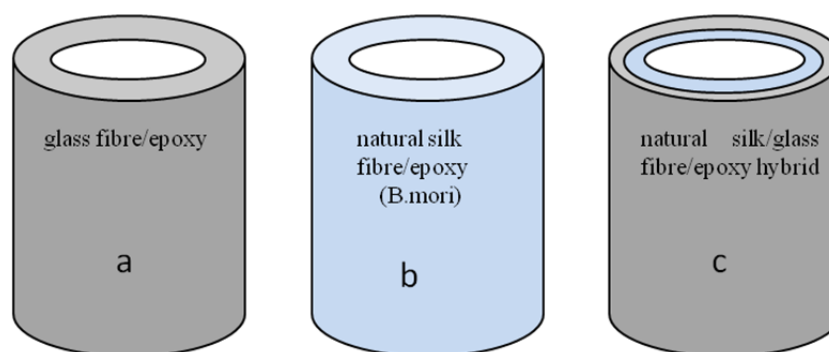


Figure 2. Schematics diagram of the specimen used (a) glass fibre/epoxy, (b) natural silk/epoxy, and (c) natural silk/glass fibre/epoxy hybrid.

2.1. The testing machine

The machine used to perform the experiment was an automated INSTRON MTS 810 universal testing machine, with loading capacity of 250 kN. The crosshead speed was kept constant at 20 mm/min throughout the experiment. Two rectangular flat plates as fixtures mounted in opposite direction were used to perform the test. Data generated during the test were collected from the computerized system and further analyzed.

3. Results and discussions

The results obtained from the tests conducted in this study were displayed and discussed here. The load-displacement curves results are presented from the average results of three tests, owing to the fact that the fracture energy is much dependent on the specific failure mechanism which can vary

from test to test even if all parameters are unvaried. Three specimens were tested from each composite configuration and their average values recorded. Figures 3a–d, 4a–e, 5a–d, show case photographs of failure fragmentation captured during the quasi-static laterally compressed load test of the composite specimens. Figures 3e, 4f, 5e show the load/displacement and energy curves obtained from the experimental tests. In Figures 7–10, the bar-chart was used for comparison analysis of characteristics like, peak load, energy absorption capability, crushing force efficiency and other features measured during the experimental test.

3.1. Deformation modes

As shown in Figures 3a–d, 4a–e, 5a–d, deformations were initiated from any of the four cardinal points of the cylindrical tube marked A, B, C and D as shown in Figure 3a. Figures 3e, 4f, 5e show the corresponding load/displacement and energy curves of the investigated composite cylindrical tubes.

3.1.1. Glass fibre/epoxy composite tube lateral load behaviour

Analyzing the deformation in Figure 3a–d, by referring to locations A, B, C and D, observations show that the two halves ACB and ADB of the cylindrical tubes undergo identical deformation, rising to the formation of elastic hinges under the load at points A, B, C and D respectively. This phenomenon is attributed to the stress built-up on those points due to compression load induced on the composite tube by the quasi-static load testing plates. As the compression load continues, the composite tube tends to deform symmetrically, with the loaded opposite sides C and D deforming inward and the other opposite sides A and B deforming outward. This report agrees partially with an observation reported by Abosbaia et al. [14]. Figure 3d, showed the final collapse nature as two adjacent eyes shape, a similar failure mode shape was observed by Abdewi et al. [11] who also worked with woven roving glass fibre/epoxy laminated composite tube.

Figure 3e displays the typical load-displacement deformation curve and failure mechanism history as well as energy absorption curve of glass fibre/epoxy composite tube under lateral quasi-static compression test. Observation show that the load maintained an increasing linear progression until it reaches the first peak load at 6.8 kN and 5.28 mm displacement. The first peak load corresponds to initiation of failure in the composite tube and marking an end to linear increase, in this case, micro to macro cracks, as seen in Figure 3b. It is good to note a slight shift observed on the load curve just before a drop in load was finally observed. This behaviour was attributed to matrix micro cracks and reloading response of reinforced fibre composites. Once the first peak load was attained, a slight drop in load associated with macro cracking failure at the four cardinal points was observed. The second peak load which is slightly higher than the first was as a result of fibre reloading, the matrix transfers the load to the reinforcing component, in this case glass fibres which sustained the load before finally breaking at a peak load of 8.76 kN and approximately 11.93 mm displacement. It was observed that the energy-displacement curve increased slightly nonlinear until it reaches 98.99 J at 18.27 mm displacement. It then maintained a low energy absorption until it reaches 100.05 J at 23.4 mm displacement.

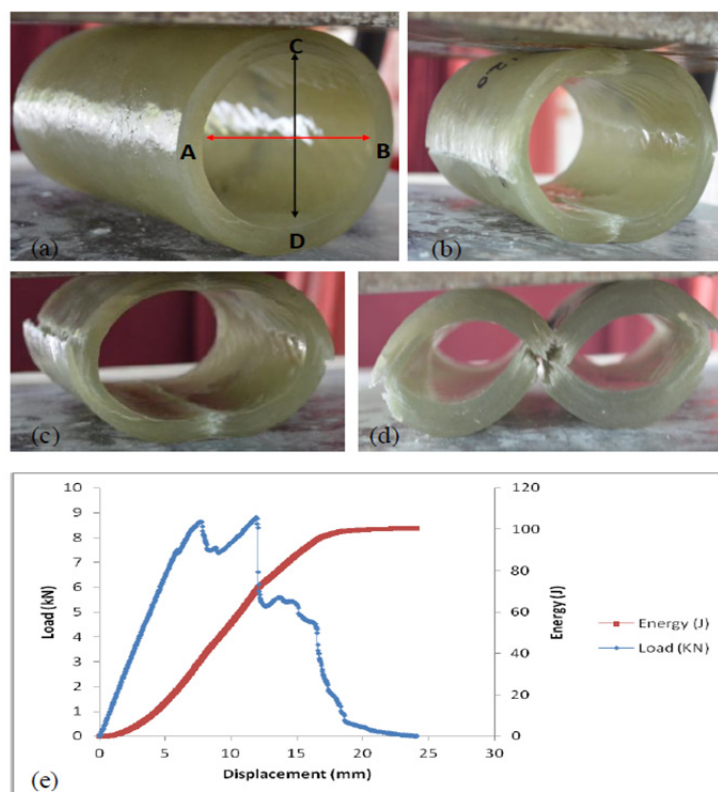


Figure 3. Glass–fibre/epoxy composite tube (a)–(d) photo of the tube deformation, (e) load-displacement and energy absorption curve.

3.1.2. Bombyx mori/epoxy composite tube lateral load behaviour

Figure 4a–e displays the result of the quasi-static lateral compressive load test of bombyx mori/epoxy composite tube. The four points A, B, C and D introduced to help analyze the lateral deformation in the previous figure under glass–fibre composite tube was also applied here to help explain the results of the present composite tube. As seen in Figure 4c, the bombyx mori/epoxy composite tube showed a symmetrical deformation; elastic hinges under load were first observed at C and D, as the compressive deformation progressed, slight elastic hinges were also seen at point A and B. At this stage observation also shows that the structure formed two similar shapes like an eye adjacent to each other. This observation continued until complete crushing of the structure was attained, compaction of the upper and lower half of the composite cylindrical tube was also observed. The failure behavior agrees to a similar failure mode observed and reported by Abdewi et al. [11].

In Figure 4f, the load-displacement deformation curve gives an interpretation of the behaviour of bombyx mori/epoxy composite tube under lateral compressive load. The curve showed a very close similarity with the typical stress-strain deformation curve of ductile materials, reflecting the ductile nature of bombyx mori silk. First peak load was assumed to occur at 0.59 kN and 10.46 mm displacement, followed by a neatly formed arc shape, which further expressed the ductility of the material under investigations. Further increase noticed in the load-displacement profile was as a result of reloading effect of the reinforced composite tube, the second peak load occurred at approximately 0.88 kN and 49 mm displacement respectively. Observation show that the energy-

displacement curve of bombyx mori/epoxy composite tube under lateral compressive load continued a nonlinear increase until it reaches 30.5 J energy absorption at 50.7 mm displacement.

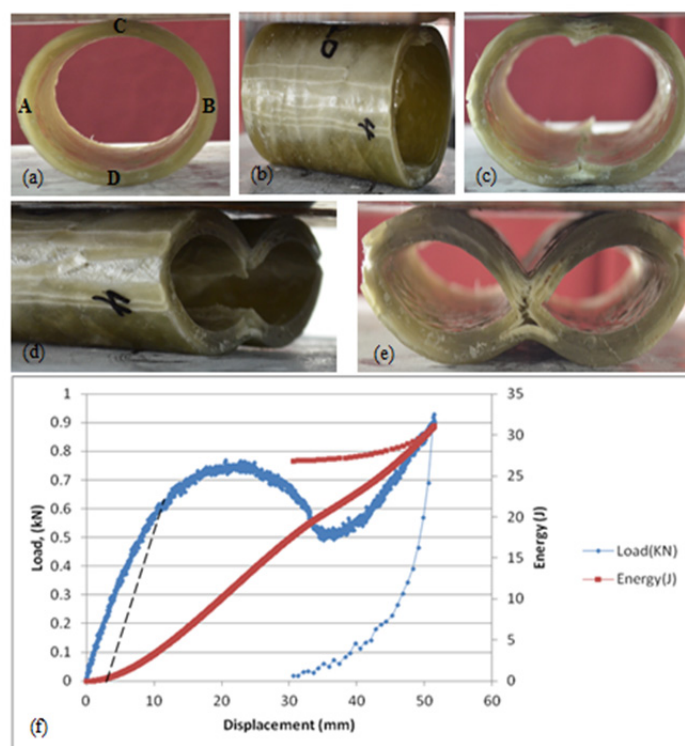


Figure 4. Bombyx mori fibre/epoxy composite tube (a)~(e) photo of the tube deformation, (f) load-displacement and energy absorption curve.

3.1.3. Bombyx mori/glass-fibre/epoxy hybrid composite tube lateral load behaviour

Figure 5 show the response of bombyx mori/glass-fibre/epoxy hybrid composite under lateral compressive load. Hybrid reinforced composite are those composites which have a combination of two or more reinforcement fibres or particulates whether in nano, micro or macro sizes. Hybrid composite are formed with predetermined intentions to utilize the strength of each individual fibre and produce a hybrid composite with better properties compared to any of the individual constituent or its composites. In the current investigation, bombyx mori fibre has an excellent ductility and elasticity properties. It is among the best natural fibres with good tensile property. Glass fibre on the other hand has a very good compression strength property, but has poor tensile property and very brittle. It is in-view of these individual excellent properties that the hybridization idea was build upon.

The deformation mode observed in Figure 5a-d shows that the ACB which formed the upper half of the cylinder and ADB the bottom part of the cylinder, deformed in dissimilar manners. It was evidence that ACB half of the cylinder collapsed into ADB half of the cylinder; elastic hinges were formed at points A, C and B; delamination and crack failures were seen on the bottom half of the cylindrical surface (see Figure 5b-d). The failure fragmentation mode was slightly deferent from the previous two observations; the combine synergy of the individual materials properties was responsible for the failure mode observed. In Figure 5e, it shows that the crushing load increased

linearly until it reaches the highest peak load value of 31.9 kN at 5.3 mm displacement. A drop in the load curve was observed immediately after the peak load was attained, signaling that a major deformation has taken place within the cylindrical hybrid composite tube. A reloading effect was seen as the curve tends to rise, but further deformation led to other significant drops in the load curve till it finally reaches the last lower peak load of 20.7 kN at 9.95 mm displacement. The energy-displacement curve on the hand increased linearly at a fast rate until it reached 197.5 J and a slow increase was observed till it reached 229.7 J. The report agrees with Cihan et al. [21] report on the woven flax/e-glass hybrid composite, who also reported that hybridization gives rise to the development of new material properties. It was evident that the hybrid composite tube outperformed the other two composite tubes both in load carrying capacity and energy absorption capability when compared.

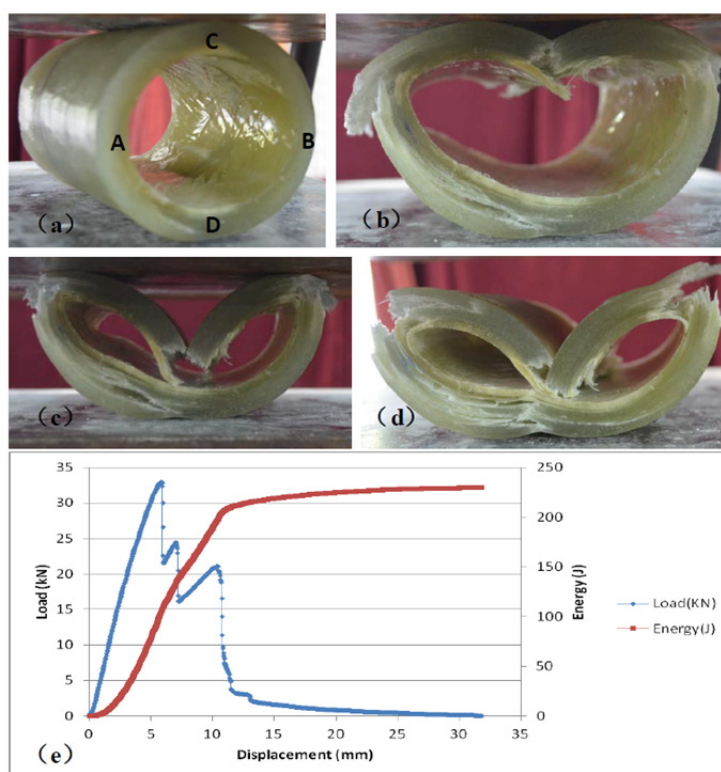


Figure 5. Bombyx mori fibre/glass-fibre/epoxy hybrid composite tube (a)~(d) photo of the tube deformation, (e) load-displacement and energy absorption curve.

3.2. Crashworthiness characteristics

The crashworthiness characteristics of any structure could be estimated by knowing different parameters, these parameters are estimated and illustrated in the below sections.

3.2.1. Crushing energy absorption behaviour

The energy absorption capability can be estimated using total energy absorption (E_t) and specific energy absorption (E_s). Total energy absorbed could be estimated as the area under the load-

displacement curve. This parameter is a function of materials density and the cross-sectional area of the specimen under investigation. The value of the energy could be obtained from the numerical integration of the load displacement curve. A comparison of the investigated tubes shows that, hybrid composite tube had a better energy absorption capability than the other tubes, see Figure 6.

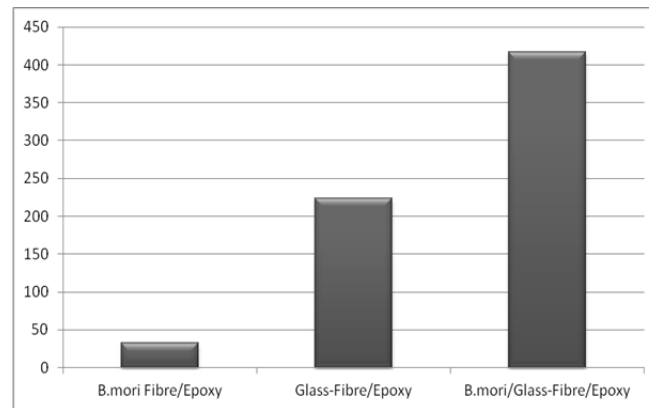


Figure 6. Absorption of energy comparisons (J) of B.mori–fibre, glass–fibre and hybrid/epoxy composite cylindrical tubes.

Specific energy absorption on the other hand is defined as the amount of energy absorbed per unit mass of crushed material. It is a vital parameter when comparing the energy capability of different materials or different specimen geometry. Figure 7 shows the specific energy absorption behavior of the three composite investigated, the hybrid composite tube clearly outperformed the other tubes. Specific energy absorption (E_s) can be estimated mathematically as Eq 1,

$$E_s = \frac{P_{avg}}{A\rho} \quad (1)$$

where P_{avg} refers to average load, A is the cross-sectional area of tube under investigation, and ρ stands for the density of the composite tube.

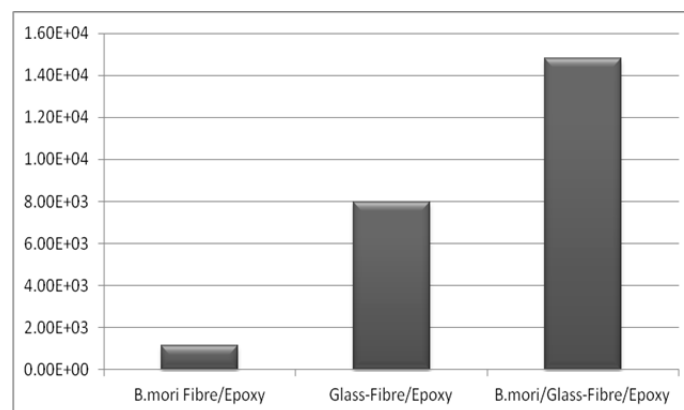


Figure 7. Specific energy absorption comparisons (J) of B.mori–fibre, glass–fibre and hybrid/epoxy composite cylindrical tubes.

3.2.2. Peak and average load behaviour

The peak load of reinforced composite structure is the maximum carriability load which the structure was able to withstand before it deformed as captured in Figure 8. Reports from the literatures [1,11,22] stated that this parameter is influenced by both the material properties of the laminates used, and the geometric parameters of the composite structure. On the other hand, the average peak load (Figure 9) is also a very vital parameter to properly define the energy absorption capability of the reinforced composite structures. It is therefore of paramount important that we investigate and understand the changes which occurs within the average loads. A comparison of the present structures under investigation show that B.mori/glass/epoxy hybrid composite tube had a higher value of 45.16 kN to outperform the other structures with 17.23 and 0.93 kN respectively. The distribution of the average load values was similar to that of the peak load, with the hybrid composite structure also having a higher value than the other two structures. The evidence before us in this investigation has again proven that hybridization improves some crashworthiness parameters like loads and energy attenuations.

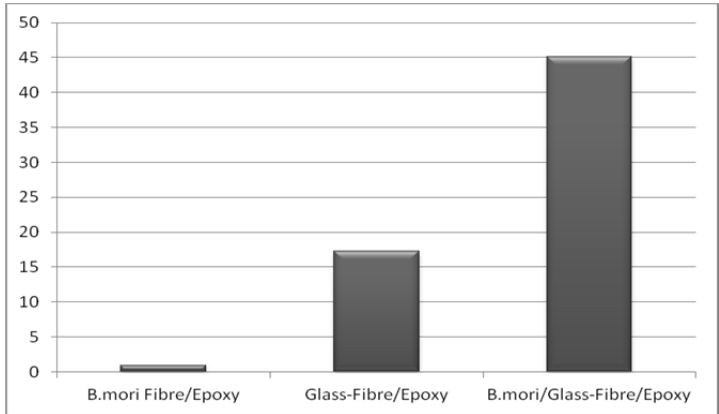


Figure 8. Peak load comparisons (kN) of B.mori–fibre, glass–fibre and hybrid/epoxy composite cylindrical tubes.

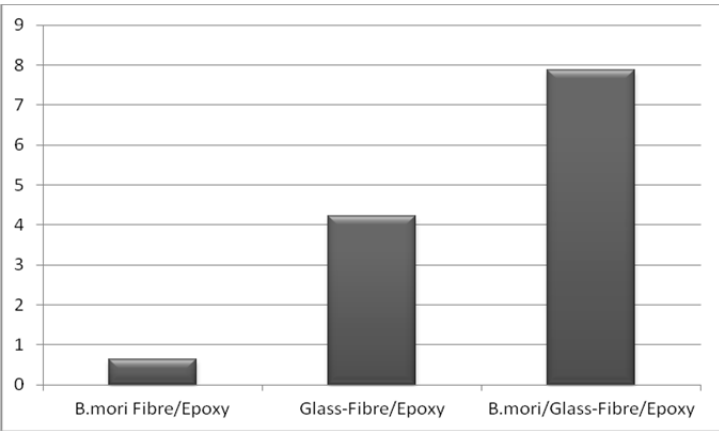


Figure 9. Average load comparisons (kN) of B.mori–fibre, glass–fibre and hybrid/epoxy composite cylindrical tubes.

3.2.3. Crush force efficiency (CFE)

Crushing force efficiency (CFE) is measured as the ratio between average crushing and initial crushing failure of the composite tubes. This parameter is useful when measuring the performance of absorbers like the tubes under investigation. It is expressed mathematically as Eq 2,

$$CFE = \frac{P_{avg}}{P_{max}} \quad (2)$$

where P_{max} and P_{avg} are the maximum initial crushing load and average crushing load, respectively. This parameter Figure 10 shows that B.mori fibre/epoxy composite tube performed better than the other tubes when compared.

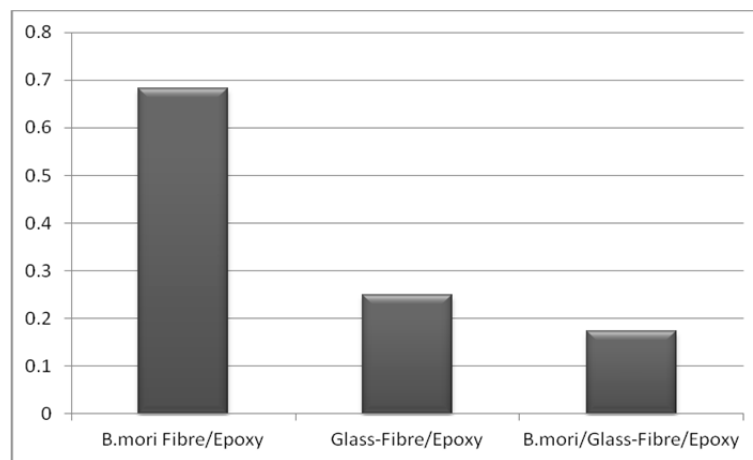


Figure 10. Crush force efficiency comparisons of B.mori–fibre, glass–fibre and hybrid/epoxy composite cylindrical tubes.

4. Fragmentation behaviour after compressive loading

Fragmentation in composite structure under compressive loads begins to occur when the applied load exceeds the elastic limit of the structure. If a structure is loaded in a way that the stresses at every point is within the elastic limit, visible deformation may not be seen as they are in very micro level, the stresses at this point are proportional to applied load. With increase in the applied load above the elastic limit, micro-macro cracks are initiated in the composite structure signaling onset of deformation. The regions where these cracks were noticed first are regions where the local stress built-up has reached the maximum capacity the structure can carry. In the present study, all three structures initiated cracks from ABC or D points, as shown previously in Figure 3a–d. The local stress increased at these points as the load is further increased. The recovery capabilities of the structures were also investigated; B.mori composite tube displayed a high degree of recovery after the load was removed. This behaviour is attributed to the ductility property of bombyx mori natural silk laminates, see Figure 11a–c.

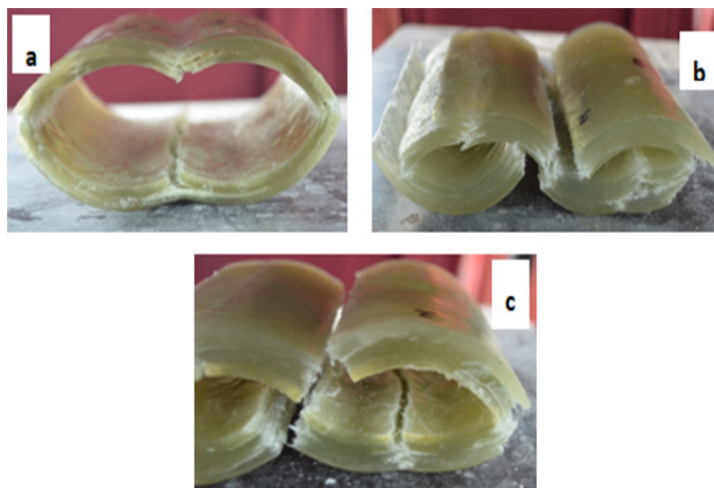


Figure 11. Reloading response after quasi-static loading (a) bombyx mori/epoxy tube (b) glass–fibre tube (c) hybrid composite tube.

5. Conclusion

In this study, investigation of the behaviour of B.mori, glass and hybrid/epoxy fibres laminated composite tubes deformed laterally have been carried out experimentally under quasi-static laterally compressive load and below were the conclusions based on the results obtained from the test.

- A comparison of the three categories of cylindrical composite tubes investigated in this study has further shown that hybridization of reinforcement fibres can indeed produce materials with better properties in comparison with their individual composites.
- B.mori/epoxy composite tube performed better in crush force efficiency and rate of recovery after compression, this may be attributed to the ductile nature of B.mori natural silk.
- Failure mechanism was mainly micro to macro cracks due to induced stresses rising from continuous quasi-axial compressive load.

Acknowledgments

The authors are supported by the funding from the research fund of the Botswana International University of Science and Technology Palapye. University initiation grants No. R00073.

Conflict of interests

The authors would like to state that there is no conflict of interests. Email: udea@biust.ac.bw; husna.azhari@ukm.eng.

References

1. Mamalis AG, Manolakos DE, Ioannidis MB, et al. (2004) Crashworthy characteristics of axially statically compressed thin-walled square CFRP composite tubes: experimental. *Compos Struct* 63: 347–360.

2. Ude AU, Ariffin AK, Azhari CH (2013) Impact damage characteristics in reinforced woven natural silk/epoxy composite face-sheet and sandwich foam, coremat and honeycomb materials. *Int J Impact Eng* 58: 31–38.
3. Ude AU, Eshkoo RA, Azhari CH (2017) Crashworthy characteristics of axial quasi-statically compressed bombyx mori composite cylindrical tubes: experimental. *Fiber Polym* 18: 1594–1601.
4. Supian ABM, Sapuan SM, Zuhri MYM, et al. (2018) Hybrid reinforced thermoset polymer composite in energy absorption tube application: A review. *Def Technol* 14: 291–305.
5. Eshkoo RA, Ude AU, Oshkoo SA, et al. (2014) Failure mechanism of woven natural silk/epoxy rectangular composite tubes under axial quasi-static crushing test using trigger mechanism. *Int J Impact Eng* 64: 53–61.
6. Eshkoo RA, Ude AU, Sulong AB, et al. (2015) Energy absorption and load carrying capability of woven natural silk epoxy-triggered composite tubes. *Compos Part B-Eng* 77: 10–18.
7. Eshkoo RA, Oshkoo SA, Sulong AB, et al. (2013) Effect of trigger configuration on the crashworthiness characteristics of natural silk epoxy composite tubes. *Compos Part B-Eng* 55: 5–10.
8. Eshkoo RA, Oshkoo SA, Sulong AB, et al. (2013) Comparative research on the crashworthiness characteristics of woven natural silk/epoxy composite tubes. *Mater Des* 47: 248–257.
9. Cormier JR, LaPlante G (2018) Study of the effects of low-velocity impact on a composite bicycle down tube. *Compos Struct* 198: 144–155.
10. Kathiresan M, Manisekar K (2017) Low velocity axial collapse behavior of E-glass fiber/epoxy composite conical frusta. *Compos Struct* 166: 1–11.
11. Abdewi EF, Sulaiman S, Hamouda AMS, et al. (2008) Quasi-static axial and lateral crushing of radial corrugated composite tubes. *Thin Wall Struct* 46: 320–332.
12. Fan Z, Shen J, Lu G (2011) Investigation of lateral crushing of sandwich tubes. *Procedia Eng* 14: 442–449.
13. Mahdi ES, El Kadi H (2008) Crushing behavior of laterally compressed composite elliptical tubes: experiments and predictions using artificial neural networks. *Compos Struct* 83: 399–412.
14. Abosbaia AS, Mahdi E, Hamouda AMS, et al. (2005) Energy absorption capability of laterally loaded segmented composite tubes. *Compos Struct* 70: 356–373.
15. Sebaey TA, Mahdi E (2016) Crashworthiness of pre-impacted glass/epoxy composite tubes. *Int J Impact Eng* 92: 18–25.
16. Moeinifard M, Liaghat G, Rahimi G, et al. (2016) Experimental investigation on the energy absorption and contact force of unstiffened and grid-stiffened composite cylindrical shells under lateral compression. *Compos Struct* 152: 626–36.
17. Ali AM, Robillard D, Masmoudi R, et al. (2019) Experimental investigation of bond and tube thickness effect on the flexural behavior of concrete-filled FPR tube under lateral cyclic loading. *J King Saud Univ Eng Sci* 31: 32–41.
18. Elahi SA, Rouzegar J, Niknejad A, et al. (2017) Theoretical study of absorbed energy by empty and foam-filled composite tubes under lateral compression. *Thin Wall Struct* 114: 1–10.
19. Liu Q, Xu X, Ma J, et al. (2017) Lateral crushing and bending responses of CFRP square tube filled with aluminum honeycomb. *Compos Part B-Eng* 118: 104–115.

20. Pol MH, Golshan NR (2019) Experimental investigation of parameters affected on behavior of composite tubes under quasi static and dynamic axial loading. *Compos Part B-Eng* 163: 471–486.
21. Cihan M, Sobey A, Blake JIR (2019) Mechanical and dynamic performance of woven flax/E-glass hybrid composites. *Compos Sci Technol* 172: 36–42.
22. Mamalis AG, Manolakos DE, Ioannidis MB, et al. (2005) On the response of thin-walled CFRP composite tubular components subjected to static and dynamic axial compressive loading: experimental. *Compos Struct* 69: 407–420.



AIMS Press

© 2019 the Author(s), licensee AIMS Press. This is an open access article distributed under the terms of the Creative Commons Attribution License (<http://creativecommons.org/licenses/by/4.0>)